Macromolecules

COMMUNICATION TO THE EDITOR

pubs.acs.org/Macromolecules

Synthesis and Ordered Phase Separation of Imidazolium-Based Alkyl−Ionic Diblock Copolymers Made via ROMP

Erin F. Wiesenauer,[†] Julian P. Edwards,[†] Vincent F. Scalfani,[‡] Travis S. Bailey,[*,‡] and Douglas L. Gin[*,†]

[†]Department of Chemistry and Biochemistry, University of Colorado, Boulder, Colorado 80309-0215, United States

[‡]Department of Chemical and Biological Engineering and Department of Chemistry, Colorado State University, Fort Collins, Colorado 80523-1370, United States

Supporting Information

Polymerized ionic liquids (poly(IL)s) are a new class of polyelectrolytes that are valuable for a number of engineering applications.[1] These cationic polymers are typically made via the covalent polymerization of imidazolium-based organic salt monomers that are liquids at ≤100 °C.[1] Imidazolium-based poly(IL)s are particularly useful as functional materials because of their unique combination of physical properties, such as high intrinsic CO_2 gas solubility and ion conductivity.[1] Consequently, these poly(IL)s have been applied as new membrane materials for separating CO_2 from other light gases,[2] as solid-state ion conductors,[3] as specialty dispersants/surfactants,[4] and as platforms for electrochemical devices,[5] to name just a few. Unfortunately, imidazolium-based poly(IL)s have only been synthesized in a limited number of polymer architectures so far. The majority of examples have been linear side-chain homopolymers (including side-chain liquid-crystalline (LC) derivatives).[1] Only a handful of examples of other homopolymer architectures (e.g., main-chain polymers;[6] amorphous[7] and ordered (LC)[8] cross-linked networks) and copolymer architectures (e.g., random[9] and blocky[10]) have been reported. Since differences in polymer architecture and composition often lead to different physical properties and morphologies, this represents an opportunity to explore and synthesize new imidazolium poly(IL)s with potentially enhanced performance in the aforementioned applications.

Phase-separated block copolymers (BCPs) represent an interesting polymer architecture for exploration of new imidazolium-based poly(IL) materials, especially for gas and ionic transport applications. Prior work with conventional, nonionic, phase-separated diblock copolymers have shown that orientation of the ordered phases can affect light gas transport.[11] If constructed with ionic blocks, copolymers with anisotropic ion-conducting domains may be produced, similar to the LC side-chain poly(IL) electrolytes described in the literature.[1] An added benefit of BCPs is that their chemical composition can be altered to obtain different mechanical properties and morphologies and incorporate the ability to selectively transport a secondary solute, without affecting the basic properties of the individual domains. In contrast, composition changes in alternating and random copolymers often result in dilution or significant modification of the overall polymer properties. Prior work documenting the solution[12−15] and melt-state[16−18] assembly of BCPs containing an ionic component have primarily focused on more traditional polyelectrolyte systems, such as those containing acrylic acid,[12−15] sulfonated styrene,[16−18] or protonated lysine residues.[13,14] However, the demonstrated formation of phase-separated ordered nanostructures in a solvent-free melt state by poly(IL)-containing BCPs is largely unprecedented. This is particularly true for the very few examples of imidazolium-containing BCPs reported in the literature so far.[10]

Herein, we present a new type of imidazolium-based, alkyl−ionic diblock copolymer (**1**) synthesized using living ring-opening metathesis polymerization (ROMP) that forms ordered nanostructures via phase separation in the solvent-free melt state at 25 °C (Figure 1). Control of the relative composition and molecular weights of the hydrophobic alkyl and imidazolium blocks in these BCPs afforded initial compositions of **1** (i.e., samples **1a**−**c** with block ratios of 1:0.90 to 1:0.42 (alkyl:imidazolium repeat units); total polymer length: 50 repeat units) that all exhibit phase separation and form highly periodic lamellar phases. Furthermore, in solution, these alkyl−imidazolium diblock copolymers all show surfactant behavior in several nonaqueous solvents. Control experiments with physical blends of the two homopolymers do not show this ordered phase separation in the melt state nor surfactant behavior in solution.

Imidazolium BCPs **1a**−**c** were synthesized via sequential living ROMP of hydrophobic alkyl monomer **2** and cationic imidazolium IL monomer **3** using Grubbs' first-generation olefin metathesis catalyst in CH_2Cl_2 solution as shown in Figure 1 (see the Supporting Information for details).[19] Monomers **2** and **3** were both synthesized from commercially available starting materials in relatively high yields (see Supporting Information). ROMP was the desired polymerization technique for making phase-separated alkyl−imidazolium BCPs due to its living and linear character, precise molecular weight control, low polydispersity (PDI), and tolerance of a diverse range of functional groups, including imidazolium units.[20] Norbornene derivatives are ideal monomers for ROMP because of their facile synthesis and modularity for functional group attachment as well as their relatively high ring strain (27.2 kcal/mol, the relief of which drives the ROMP reaction).[21] In our block copolymerizations, **2** was first polymerized to form an initial hydrophobic block, followed by living addition of **3** to form the subsequent ionic block. This order of copolymerization was used because the living polymerization of monomer **2** proceeds faster than the

Received: January 26, 2011
Revised: June 1, 2011
Published: June 15, 2011

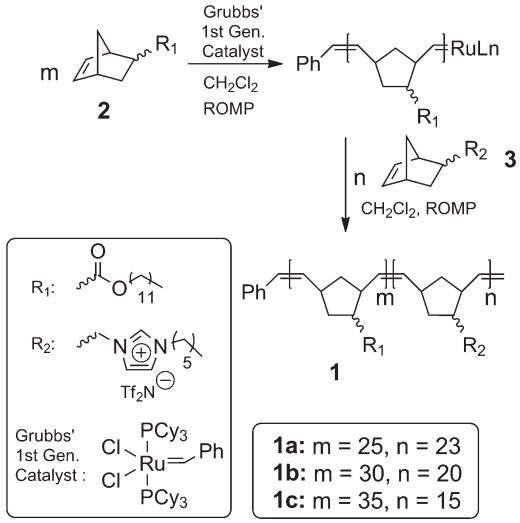

Figure 1. Synthesis and structures of alkyl−imidazolium diblock copolymers **1a**−**c** made via ROMP that show ordered phase separation in the melt state. The values of *m* and *n* depicted in **1a**−**c** are derived from the observed NMR block length ratios of the BCPs and the monomer-to-catalyst ratios as used in the living ROMP of **2** and **3**.

ionic monomer **3** (ca. 3−4 times faster at room temperature). By varying the molar ratios of **2** and **3** in the sequential ROMP reactions, alkyl−imidazolium BCPs with different alkyl vs imidazolium block length ratios were successfully formed.

The ability to polymerize monomers **2** and **3** sequentially to afford BCPs **1a**−**c** with distinct block composition ratios and lengths was confirmed by ^{1}H NMR analysis on the polymers and experimental confirmation of living ROMP behavior for the two monomers. The alkyl:imidazolium repeat unit molar ratios for each BCP prepared were directly determined by integrating and comparing distinct ^{1}H NMR signals indicative of each block. The block lengths (Figure 1) were then calculated from the NMR-based repeat unit ratios and the copolymerization monomer-to-catalyst ratios, after confirming living ROMP homopolymerization character for each monomer (see the Supporting Information for details).[22] The M_n values for BCPs **1a**−**c** were then approximated by multiplying the calculated block lengths by the repeat unit molecular weights. The approximate M_n values for **1a**, **1b**, and **1c** are 20 100, 20 000, and 18 800 g/mol, respectively (see Supporting Information). The absolute M_n values for the BCPs **1a**−**c** could not be determined directly using ^{1}H NMR end-group analysis as in the case of the individual homopolymers because the imidazolium proton signals are shifted slightly in the BCPs and overlap with the five phenyl end-group protons. Unfortunately, conventional methods used to typically determine the molecular weight, molecular weight distribution, and block architecture of copolymers (e.g., GPC, matrix-assisted laser desorption ionization time-of-flight mass spectrometry, and dynamic light scattering) were attempted on **1a**−**c**, but all yielded inconclusive results. These difficulties were largely associated with the challenges inherent in the characterization of such highly charged macromolecules.[1] Since the block architecture of **1a**−**c** could not be determined using conventional polymer molecular weight characterization methods, a combination of alternative methods was used to verify a block architecture and to differentiate their behavior from that of a simple physical blend of homopolymers of **2** and **3**. These alternative methods included surfactant behavior and solubility analysis, diffusion-ordered spectroscopy (DOSY), differential scanning calorimetry (DSC), rheological measurements, and small-angle X-ray scattering (SAXS) studies.

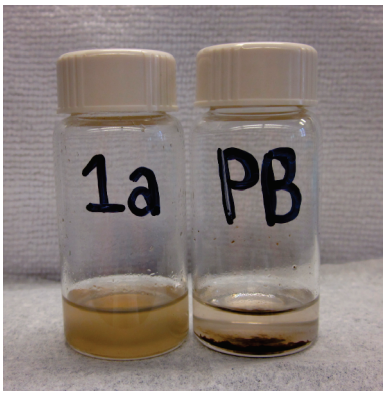

Figure 2. Different solubilities of copolymer **1a** and a physical blend (PB) of poly(**2**) + poly(**3**) in hexanes at room temperature.

With respect to surfactant and solubility behavior, it was found that copolymers **1a**−**c** all show surfactant behavior (i.e., extensive foaming when agitated) when mixed in hexanes, THF, $CHCl_3$, EtOAc, MeOH, and CH_3CN, as would be expected from amphiphilic BCPs. Control experiments with physical blends of poly(**2**) and poly(**3**) of the same length as in the copolymers do not show this behavior. Copolymers **1a**−**c** also show very different solubility behavior compared to physical blends of the two homopolymers, poly(**2**) and poly(**3**). For example, when mixed with hexanes (10 mg/mL) **1a** forms opaque heterogeneous suspensions, whereas the physical blend yields a brown solid within a clear solution on top (i.e., poly(**2**) is soluble in hexanes while poly(**3**) is insoluble) (Figure 2). Similar results were observed when comparing samples **1a**−**c** to their physical blends in ethyl acetate and acetonitrile, where poly(**3**) is soluble and poly(**2**) is insoluble.

In NMR DOSY studies, it was found that copolymer **1a** in CD_2Cl_2 (10 mg/mL) only showed one room-temperature diffusion coefficient (3.68×10^{-10} m^2/s), whereas a physical blend of the two homopolymers of comparable length exhibited two distinct diffusion coefficients (8.8×10^{-10} and 10.6×10^{-10} m^2/s). **1a** consists of only one macromolecular species and is different than the physical blend of two distinct macromolecular species. Collectively, the results of these comparative studies are consistent with a covalently linked BCP architecture for **1a**−**c**, instead of a physical blend of the two homopolymers.

Further verification of the block architecture of copolymers **1a**−**c** and their collective ability to form phase-separated structures was established via a combination of DSC, dynamic rheology, and SAXS data collection. DSC studies on samples of **1a**−**c** revealed the presence of two broad but distinct thermal transitions near −28 and 7 °C, consistent with crystallization of the *n*-dodecyl side-chains and the vitrification of the imidazolium blocks, respectively (see Supporting Information). The thermal transitions at ca. 7 °C for BCPs **1b** and **1c** exhibit decreased intensity since they are associated with smaller imidazolium block regions. These DSC results do not directly verify connectivity between the polymer blocks but do establish their phase-separated state in the melt. Slight shifts in the transition temperatures of the BCPs of several degrees relative to those of

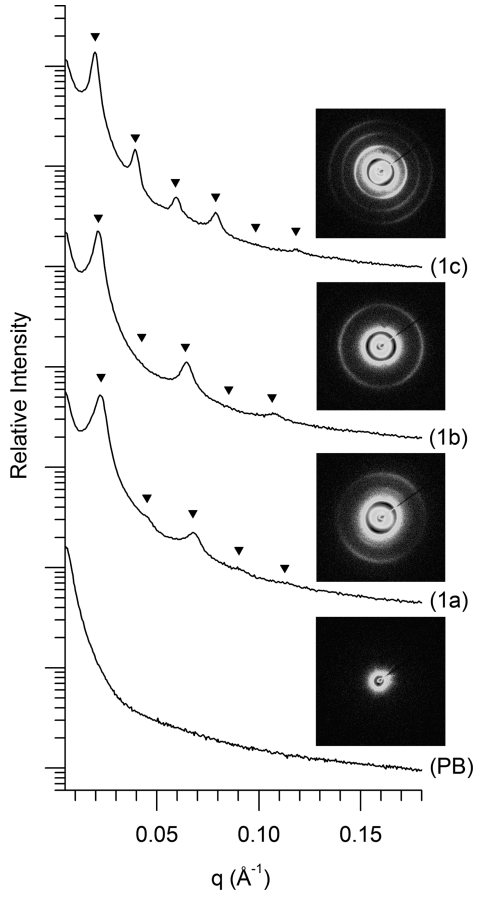

Figure 3. Representative SAXS data for imidazolium BCPs containing block ratios of 1:0.90 (**1a**), 1:0.66 (**1b**), and 1:0.42 (**1c**), with the corresponding 2D detector images (inset). Inverted triangles represent the location of the allowed reflections for the lamellar morphology, calculated based on the position of the primary scattering wave vector q_{100}: (L) q/q^* at $\sqrt{1}$, $\sqrt{4}$, $\sqrt{9}$, $\sqrt{16}$, $\sqrt{25}$, $\sqrt{36}$, etc. The physical blend (PB) of poly(**2**) and poly(**3**) shows no observable diffraction peaks, in contrast to the BCPs.

the individual homopolymers are also consistent with restricted domain sizes and finite interfacial widths typical of ordered BCP morphologies.

While the combination of solubility, NMR DOSY, and DSC confirmed the connected block structure and phase-separated state of **1a**−**c**, SAXS analysis was used to establish the length scale (and thus block connectivity) and domain geometry of the ordered melts of these samples. SAXS analysis on each of the compositionally unique BCPs verified phase separation on the nanoscale and thus block connectivity with absolute certainty. Representative 25 °C SAXS data are shown in Figure 3 for each of the alkyl−imidazolium BCPs synthesized, together with data collected for the physical blend (PB) of the two homopolymers for comparison. At each of the block ratios synthesized, prominent principal diffraction peaks plus multiple higher order reflections are consistent with melt-state lamellar (L) phase morphologies.[23] Notably, the domain spacings ($d = 2\pi/q$) for the three BCP species are very similar (**1a**: 28.6 nm; **1b**: 29.4 nm; **1c**: 32.1 nm), although increasing slightly as the composition shifts toward greater fractions of the nonionic block (poly(**2**)). Interestingly, the principal domain spacings ($d = 2\pi/q$) in the range of 30 nm are quite large compared to many traditional BCP systems, considering both the targeted degree of polymerization (∼50) and approximate average molecular weights in the 20 000 g/mol range. For comparison, a PS−PVP lamellar block copolymer of similar molecular weight would be expected to have a domain spacing around only 20 nm.[24] However, the manner in which mass is distributed along these two BCP chains is quite different, with the PS−PVP chain described above having a contour length about 60% longer than **1a**−**c**. Thus, mass (and volume) is concentrated more densely along the length of **1a**−**c** (repeat unit molecular weights of monomer **2** and **3** of 307 and 540 g/mol, respectively), resulting in stiffer, "fatter" chains that favor larger domain spacings. Notably, the mass fraction of the imidazolium block in BCPs **1a**−**c** ranges from 0.43 (**1c**) to 0.54 (**1b**) to 0.62 (**1a**) which, while difficult to accurately correlate to volume fractions without known homopolymer densities, appears highly consistent with the expected location of the L phase window exhibited by other classic BCP systems.[23] The variation in higher-order diffraction peak intensities for the three samples is also consistent with changes in composition, as the relative thicknesses of the alkyl and ionic domains making up the lamellar period directly affect the superposition product of the form (particle) and structure (lattice) factor scattering contributions. For example, the notable absence of the reflections at $q/q^* = \sqrt{4}$ and $\sqrt{16}$ in sample **1b** suggests the 1:0.66 repeat unit ratio is approaching a nearly symmetric volume fraction of 0.5, in which the minima in the form factor scattering cancels out the diffraction intensity associated with the lamellar periodicity for even-order diffraction maxima.[25] Dynamic rheological measurements on BCPs **1a**−**c** also revealed behavior prototypical of traditional lamellar BCP melts, exhibiting elastic and loss moduli of similar magnitudes, with a tendency to decrease together monotonically with increasing temperature (see Supporting Information).[23] None of the systems revealed any order−order transitions below 150 °C. Importantly, a physical blend of the two homopolymers (poly(**2**) + poly(**3**)) does not exhibit any observable scattering or diffraction, confirming the necessity of the covalent bond between the blocks for microphase separation.

In summary, a new type of imidazolium-based, alkyl−ionic BCP has been synthesized that undergoes ordered phase separation in the melt state and exhibits surfactant behavior in nonaqueous solvent. This new BCP platform is based on the sequential ROMP of alkyl− and imidazolium IL−norbornene monomers, which provides convenient block ratio and length control. Extensive control experiments indicated that the ordered phase separation of these new alkyl−imidazolium copolymers is due to a block architecture, and that these copolymers behave very differently from a physical blend of the analogous homopolymers in solution and the melt state. To our knowledge, this system is one of the first examples of a poly(IL)-containing BCP that forms phase-separated, ordered nanostructures in the melt state. We are in the process of exploring a wider range of block length ratios for this BCP system in order to map out its full phase behavior. We are also currently extending this project to new monomer systems and ROMP catalysts, testing the performance of these nanostructured imidazolium BCPs as gas separation membranes, and exploring the synthesis of imidazolium triblock copolymers.

■ ASSOCIATED CONTENT

Ⓢ Supporting Information. Details for the synthesis and chemical characterization of monomers **2** and **3**, BCPs **1a**−**c**, and homopolymers poly(**2**) and poly(**3**); procedure for estimating

M_n values of **1a**−**c** via block composition analysis and confirmation of living polymerization with predictable M_n control; comparative DSC and NMR DOSY data on **1a**−**c** and the control polymers; procedures and parameters for performing the rheology and SAXS studies. This material is available free of charge via the Internet at http://pubs.acs.org.

AUTHOR INFORMATION

Corresponding Authors

*E-mail: gin@spot.colorado.edu (D.L.G.); travis.bailey@colostate.edu (T.S.B.).

ACKNOWLEDGMENT

Primary financial support for the work performed at CU Boulder was provided by the Defense Threat Reduction Agency (Grant HDTRA1-08-1-0028) and the Advanced Research Projects Agency − Energy (Grant DE-AR0000098). E.F.W. thanks M. Moran, Dr. R. K. Shoemaker, and B. Norris for their extensive help with the DSC, DOSY NMR, and attempted GPC work. J.P. E. thanks the Undergraduate Research Opportunities Program at CU Boulder for support of his work in this effort. Primary financial support for the work performed at CSU was provided by the National Science Foundation (Grant DMR-0645781). SAXS studies were performed at CSU using a regional instrument supported by National Science Foundation MRI Program (Grant DMR-0821799).

REFERENCES

(1) For a comprehensive review of poly(IL)s and their applications, see: (a) Green, O.; Grubjesic, S.; Lee, S.; Firestone, M. A. *J. Macromol. Sci., Part C: Polym. Rev.* **2009**, *43*, 339. (b) Green, M.; Long, R. *J. Macromol. Sci., Part C: Polym. Rev.* **2009**, *49*, 291. (c) Lu, J.; Yan, F.; Texter, J. *Prog. Polym. Sci.* **2009**, *34*, 431. (d) Anderson, E.; Long, T. *Polymer* **2010**, *51*, 2447. (e) Jaeger, W.; Bohrisch, J.; Laschewsky, A. *Prog. Polym. Sci.* **2010**, *35*, 511.

(2) For leading examples of poly(IL)s as membrane materials for CO_2 separations, see: (a) Ding, S.; Tang, H.; Radosz, M.; Shen, Y. *J. Polym. Sci., Part A: Polym. Chem.* **2004**, *42*, 5794. (b) Bara, J. E.; Lessmann, S.; Gabriel, C. J.; Hatakeyama, E. S.; Noble, R. D.; Gin, D. L. *Ind. Eng. Chem. Res.* **2007**, *46*, 5397.

(3) For leading examples of poly(IL)s as ion conductors, see: (a) Ohno, H.; Ito, K. *Chem. Lett.* **1998**, *27*, 751. (b) Ohno, H.; Yoshizawa, M.; Ogihara, W. *Electrochim. Acta* **2004**, *50*, 255. (c) Vygodskii, Y.; Shaplov, A.; Lozinskaya, E.; Lyssenko, K.; Golovanov, D.; Malyshkina, I.; Gavrilova, N.; Buchmeiser, M. *Macromol. Chem. Phys.* **2008**, *209*, 40.

(4) For leading examples of poly(IL)s as dispersants and surfactants, see: (a) Marcilla, R.; Curri, M. L.; Cozzoli, P. D.; Martínez, M. T.; Loinaz, I.; Grande, H.; Pomposo, J. A.; Mecerreyes, D. *Small* **2006**, *2*, 507. (b) Fukushima, T.; Kosaka, A.; Yamamoto, Y.; Aimiya, T.; Notazawa, S.; Takigawa, T.; Inabe, T.; Aida, T. *Small* **2006**, *2*, 554.

(5) For leading examples of poly(IL)s used in electrochemical devices, see: (a) Ho, H. A.; Leclerc, M. *J. Am. Chem. Soc.* **2003**, *125*, 4412. (b) Ricks-Laskoski, H. L.; Snow, A. W. *J. Am. Chem. Soc.* **2006**, *128*, 12402.

(6) (a) Suzuki, K.; Yamaguchi, M.; Hotta, S.; Tanabe, N.; Yanagida, S. *J. Photochem. Photobiol. A: Chem.* **2004**, *164*, 81. (b) Li, F.; Cheng, F.; Shi, J.; Cai, F.; Liang, M.; Chen, J. *J. Power Sources* **2007**, *165*, 911. (c) Liang, Z. Y.; Lu, C. X.; Luo, J.; Dong, L. B. *J. Fluorine Chem.* **2007**, *128*, 608.

(7) (a) Muldoon, M. J.; Gordon, C. M. *J. Polym. Sci., Part A: Polym. Chem.* **2004**, *42*, 3865. (b) Nakajima, H.; Ohno, H. *Polymer* **2005**, *46*, 11499. (c) Marcilla, R.; Sanchez-Paniagua, M.; Lopez-Ruiz, B.; Lopez-Cabarcos, E.; Ochoteco, E.; Grande, H.; Mecerreyes, D. *J. Polym. Sci., Part A: Polym. Chem.* **2006**, *44*, 3958. (d) Bara, J. E.; Hatakeyama, E. S.; Gabriel, C. J.; Lessmann, S.; Gin, D. L.; Noble, R. D. *J. Membr. Sci.* **2008**, *316*, 186.

(8) Yoshio, M.; Kagata, T.; Hoshino, K.; Mukai, T.; Ohno, H.; Kato, T. *J. Am. Chem. Soc.* **2006**, *128*, 5570.

(9) (a) Zhang, G.; Liu, X.; Li, B.; Bai, Y. *J. Appl. Polym. Sci.* **2009**, *112*, 3337. (b) Tan, R.; Yin, D.; Yu, N.; Zhao, H.; Yin, D. *J. Catal.* **2009**, *263*, 284.

(10) (a) Stancik, C. M.; Lavoie, A. R.; Schutz, J.; Achurra, P. A.; Lindner, P.; Gast, A. P.; Waymouth, R. M. *Langmuir* **2004**, *20*, 596. (b) Vijayakrishna, K.; Jewrajka, S. K.; Ruiz, A.; Marcilla, R.; Pomposo, J. A.; Mecerreyes, D.; Taton, D.; Gnanou, Y. *Macromolecules* **2008**, *41*, 6299. (c) Mori, H.; Yahagi, M.; Endo, T. *Macromolecules* **2009**, *42*, 8082. (d) Vijayakrishna, K.; Mecerreyes, D.; Gnanou, Y.; Taton, D. *Macromolecules* **2009**, *42*, 5167. (e) Gu, Y.; Lodge, T. *Macromolecules* **2011**, *44*, 1732.

(11) Drzal, P. L.; Halasa, A. F.; Kofinas, P. *Polymer* **2000**, *41*, 4671.

(12) Annaka, M.; Morishita, K.; Okabe, S. *J. Phys. Chem. B* **2007**, *111*, 11700.

(13) Gebhardt, K. E.; Ahn, S.; Venkatchalam, G.; Savin, D. A. *Langmuir* **2007**, *23*, 2851.

(14) Naik, S. S.; Savin, D. A. *Macromolecules* **2009**, *42*, 7114.

(15) Zhang, L.; Shen, H.; Eisenburg, A. *Macromolecules* **1997**, *30*, 1001.

(16) Lu, X.; Weiss, R. A. *Macromolecules* **1993**, *26*, 3615.

(17) Park, M. J.; Balsara, N. P. *Macromolecules* **2008**, *41*, 3678.

(18) Saito, T.; Mather, B. D.; Costanzo, P. J.; Beyer, F. L.; Long, T. E. *Macromolecules* **2008**, *41*, 3503.

(19) Commercially available Grubbs' first- and second-generation olefin metathesis catalysts were tested for ROMP of **2** and **3**. Grubbs' first-generation catalyst was found to be the best catalyst of the two for this system. Other ROMP catalysts such as Grubbs' third-generation catalyst were not tested for this initial proof-of-concept study because they are not commercially available, but they will be tested in follow-up studies.

(20) (a) Bielawski, C. W.; Grubbs, R. H. *Prog. Polym. Sci.* **2007**, *32*, 1. (b) Arstad, E.; Barrett, A.; Tedeschi, L. *Tetrahedron Lett.* **2003**, *44*, 2703. (c) Vygodskii, Y.; Shaplov, A.; Lozinskaya, E.; Filippov, O.; Shubina, E.; Bandari, R.; Buchmeiser, M. *Macromolecules* **2006**, *39*, 7821. (d) Zheng, L.; Chen, F.; Xie, M.; Han, H.; Dai, Q.; Zhang, Y.; Song, C. *React. Funct. Polym.* **2007**, *67*, 19.

(21) Walker, R.; Conrad, R. M.; Grubbs, R. H. *Macromolecules* **2009**, *42*, 599.

(22) In addition, samples taken of poly(**2**) prior to the addition of **3** during the sequential ROMP polymerizations confirmed that the molecular weight distribution of poly(**2**) was symmetric and monomodal, with PDI values consistently in the 1.15−1.17 range for all samples.

(23) Hamley, I. W. *The Physics of Block Copolymers*; Oxford University Press: Oxford, 1999; p 432.

(24) Matsushita, Y.; Mori, K.; Saguchi, R.; Nakao, Y.; Noda, I.; Nagasawaid, M. *Macromolecules* **1990**, *23*, 4313.

(25) (a) Hasegawa, H.; Hashimoto, T.; Kawai, H.; Lodge, T. P.; Amis, E. J.; Glinka, C. J.; Han, C. C. *Macromolecules* **1986**, *18*, 67. (b) Hashimoto, T.; Nagatoshi, K.; Todo, A.; Hasegawa, H.; Kawai, H. *Macromolecules* **1974**, *7*, 364.